ABAQUS implementation of isotropic power-law hardening plasticity

Emilio Martínez-Pañeda[a,*]

[a]*Department of Civil and Environmental Engineering, Imperial College London, London SW7 2AZ, UK*

Abstract

Documentation that accompanies the file `UMATPlasticity.f`, a user material (UMAT) subroutine for implementing conventional von Mises plasticity with power law isotropic hardening. If using this code for research or industrial purposes, please cite:

E. Martínez-Pañeda, S. Fuentes-Alonso, C. Betegón. Gradient-enhanced statistical analysis of cleavage fracture. European Journal of Mechanics - A/Solids 77, 103785 (2019)

Keywords:
J_2 plasticity, Power law hardening, ABAQUS, UMAT subroutine, Finite element analysis

1. Introduction

The goal of this document is to provide an introduction to the use and implementation of user material (UMAT) subroutines in Abaqus. Also, it should help the reader become familiar with the concepts of implicit integration of non-linear material models and the implementation of plasticity theories into finite element codes. While conventional von Mises plasticity is available in ABAQUS as in-built capability, this example aims at: (i) enabling to directly define (without tabular data) power law isotropic hard-

*Corresponding author.
Email address: `e.martinez-paneda@imperial.ac.uk` (Emilio Martínez-Pañeda)

ening, and (ii) set the basis for the implementation of more advanced models.

The remainder of this document is organised as follows. Section 2 includes a description of the constitutive model. The details of the implicit numerical implementation are provided in Section 3. The usage of the user material subroutine (UMAT) and a representative numerical example are discussed in 4. Finally, concluding remarks are given in Section 5.

2. von Mises plasticity theory

Let us briefly describe the main features of conventional von Mises plasticity (Dunne and Petrinic, 2005). Small strains will be assumed for simplicity although the formulation can deal with both small and large deformations.

Strain decomposition. The total strains $\boldsymbol{\varepsilon}$ are additively decomposed into the elastic $\boldsymbol{\varepsilon}^e$ and plastic $\boldsymbol{\varepsilon}^p$ strain tensors

$$\boldsymbol{\varepsilon} = \boldsymbol{\varepsilon}^e + \boldsymbol{\varepsilon}^p \tag{1}$$

Incompressibility condition. Plastic deformation takes place without volume change, implying that the sum of the axial plastic strain rate components is zero:

$$\text{tr}\left(\dot{\boldsymbol{\varepsilon}}^p\right) = \dot{\varepsilon}_{11}^p + \dot{\varepsilon}_{22}^p + \dot{\varepsilon}_{33}^p = 0 \tag{2}$$

Yield condition. A yield condition is needed to determine if we are in the elastic or plastic regime. For a given material yield stress σ_y and effective stress σ_e, plasticity will take place when the following yield function is equal to zero.

$$f = \sigma_e - \sigma_y \tag{3}$$

It remains to define the effective stress σ_e. In the context of von Mises plasticity theory this is done taking into consideration that: (i) yield is independent of the hydrostatic stress, (ii) yield in polycrystalline metals can be taken to be isotropic, and (iii) the yield condition is the same for compression and tension. In von Mises plasticity the effective stress is defined assuming that yielding occurs when the distortion energy w_d reaches a critical value. w_d is the deviatoric part of the elastic strain energy density:

$$w_d = \frac{1+\nu}{2E}\text{tr}\left(\left(\boldsymbol{\sigma}'\right)^2\right) \tag{4}$$

where $\boldsymbol{\sigma}'$ is the deviatoric stress tensor, E is Young's modulus and ν is Poisson's ratio. Using the principal stress:

$$w_d = \frac{1+\nu}{6E}\left((\sigma_I - \sigma_{II})^2 + (\sigma_{II} - \sigma_{III})^2 + (\sigma_{III} - \sigma_I)^2\right) \tag{5}$$

In uniaxial tension, it reads:

$$w_d = \frac{1+\nu}{6E}\sigma_e^2 \tag{6}$$

Substituting in (3) and re-arranging we reach the yielding function:

$$f(\boldsymbol{\sigma}) = \frac{1}{\sqrt{2}}\left[(\sigma_I - \sigma_{II})^2 + (\sigma_{II} - \sigma_{II})^2 + (\sigma_{III} - \sigma_I)^2\right]^{1/2} = \sigma_y \tag{7}$$

Thus, one can define the effective stress as:

$$\begin{aligned}\sigma_e &= \sqrt{\frac{1}{2}\left[(\sigma_I - \sigma_{II})^2 + (\sigma_I - \sigma_{III})^2 + (\sigma_{II} - \sigma_{III})^2\right]} = \sqrt{\frac{3}{2}\boldsymbol{\sigma}' : \boldsymbol{\sigma}'} \\ &= \sqrt{\frac{1}{2}\left[(\sigma_{11} - \sigma_{22})^2 + (\sigma_{11} - \sigma_{33})^2 + (\sigma_{22} - \sigma_{33})^2 + 6\sigma_{12}^2 + 6\sigma_{13}^2 + 6\sigma_{23}^2\right]}\end{aligned} \tag{8}$$

<u>Plastic flow rule</u>. The normality condition tells us the "direction" of plastic flow after yield. As sketched in Fig. 1, assuming von Mises plasticity (associated flow), the increment in the plastic strain tensor is in a direction which is normal to the yield surface.

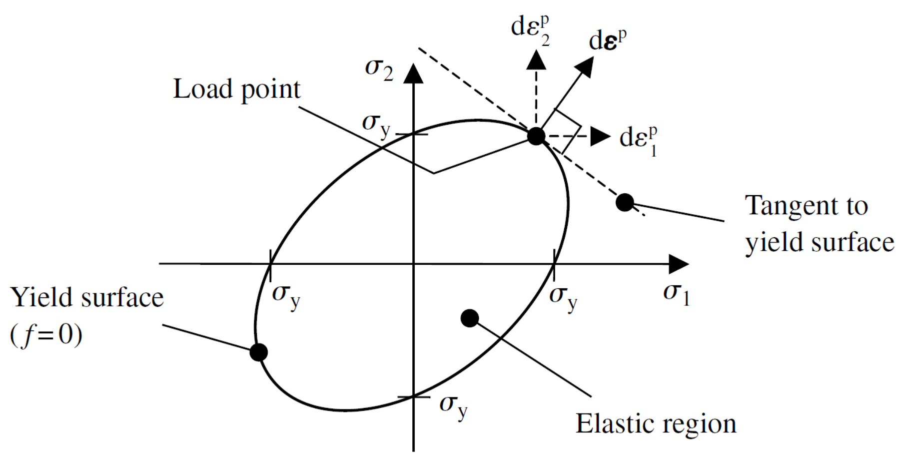

Figure 1: The von Mises yield surface for conditions of plane stress, showing the increment in plastic strain $d\boldsymbol{\varepsilon}^p$, in a direction normal to the tangent to the surface. Source: Dunne and Petrinic (2005).

The flow rule is then given as a function of the yield function f and the plastic multiplier λ:

$$\dot{\boldsymbol{\varepsilon}}^p = \dot{\lambda} \frac{\partial f}{\partial \boldsymbol{\sigma}} \tag{9}$$

where $\dot{\lambda}$ gives the magnitude of the plastic strain rate and $\partial f / \partial \boldsymbol{\sigma}$ gives the direction of the plastic strain increment. In von Mises plasticity an effective plastic strain is defined as:

$$\varepsilon_p = \sqrt{\frac{2}{3} \boldsymbol{\varepsilon}^p : \boldsymbol{\varepsilon}^p} \tag{10}$$

and accordingly the plastic flow law reads:

$$\dot{\boldsymbol{\varepsilon}}^p = \frac{3}{2} \dot{\varepsilon}_p \frac{\boldsymbol{\sigma}'}{\sigma_e} \tag{11}$$

Hardening rules. We will focus on isotropic hardening and a power law hardening rule. Specifically, the widely used form: (see, e.g., Martínez-Pañeda and Niordson, 2016; Martínez-Pañeda et al., 2016)

$$\sigma_f = \sigma_y \left(1 + \frac{E \varepsilon_p}{\sigma_y} \right)^N \tag{12}$$

where σ_f is the flow stress (or current yield stress) and N ($0 \leq N \leq 1$) is the strain hardening exponent.

3. Numerical implementation

We proceed to describe the numerical implementation aiming at correlating the equations with the steps followed in the user material subroutine. The first step involves determining the elastic trial stress. Thus, the elastic stiffness matrix is built first from the shear modulus μ and Lame's first parameter λ:

$$\boldsymbol{C} = \begin{pmatrix} 2\mu + \lambda & \lambda & \lambda & 0 & 0 & 0 \\ \lambda & 2\mu + \lambda & \lambda & 0 & 0 & 0 \\ \lambda & \lambda & 2\mu + \lambda & 0 & 0 & 0 \\ 0 & 0 & 0 & \mu & 0 & 0 \\ 0 & 0 & 0 & 0 & \mu & 0 \\ 0 & 0 & 0 & 0 & 0 & \mu \end{pmatrix} \tag{13}$$

One then proceeds to determine the elastic trial stress from the total strain increment:

$$\boldsymbol{\sigma}^{tr} = \boldsymbol{\sigma}_t + \boldsymbol{C}\Delta\boldsymbol{\varepsilon} \tag{14}$$

where $\boldsymbol{\sigma}_t$ is the Cauchy stress tensor in the previous increment. The second step is to determine the trial yield function; i.e., computing the trial effective stress:

$$\sigma_e^{tr} = \sqrt{\frac{1}{2}\left[\left(\sigma_{11}^{tr} - \sigma_{22}^{tr}\right)^2 + \left(\sigma_{11}^{tr} - \sigma_{33}^{tr}\right)^2 + \left(\sigma_{22}^{tr} - \sigma_{33}^{tr}\right)^2 + 6\left(\sigma_{12}^{tr}\right)^2 + 6\left(\sigma_{13}^{tr}\right)^2 + 6\left(\sigma_{23}^{tr}\right)^2\right]} \tag{15}$$

The flow stress (current value of the yield stress) is determined from the hardening law:

$$\sigma_f = \sigma_y \left(1 + \frac{E\left(\varepsilon_p\right)_t}{\sigma_y}\right)^N \tag{16}$$

And we determine if active yielding - is $f > 0$? Where $f = \sigma_e^{tr} - \sigma_f$. If yes, the third step is to determine the flow direction $\left(\boldsymbol{\sigma'}\right)^{tr} / \sigma_e^{tr}$ and calculate the effective plastic strain increment using the Newton method. A current tangent modulus can be defined based on the power law hardening rule, which in this case reads:

$$E_t = EN \left(1 + \frac{E\left(\varepsilon_p\right)_t}{\sigma_y}\right)^{(N-1)} \tag{17}$$

To determine the incremental equivalent plastic strain one must solve the following equation:

$$\sigma_e^{tr} - 3\mu\Delta\varepsilon_p = \sigma_f\left(\varepsilon_p\right) \tag{18}$$

Newton's method is used to minimise the residual r and find a solution for $\Delta\varepsilon_p$ following an iterative procedure. Thus, for an iteration (i):

$$r^{(i)} = \sigma_e^{tr} - 3\mu\Delta\varepsilon_p - \sigma_f \tag{19}$$

$$\Delta\varepsilon_p = \Delta\varepsilon_p^{(i)} + \frac{r}{\left(3\mu + E_t\right)} \tag{20}$$

$$\sigma_f = \sigma_y \left(1 + \frac{E\left(\varepsilon_p + \Delta\varepsilon_p\right)}{\sigma_y}\right)^N \tag{21}$$

$$E_t = EN \left(1 + \frac{E\left(\varepsilon_p + \Delta\varepsilon_p\right)}{\sigma_y}\right)^{(N-1)} \tag{22}$$

and the backward Euler iteration scheme concludes when $r \approx 0$. Once the value of $\Delta\varepsilon_p$ has been determined, one can use the normality condition to determine the stress, elastic strain and plastic strain tensors:

$$\boldsymbol{\sigma} = \frac{(\boldsymbol{\sigma}')^{tr}}{\sigma_e^{tr}} \sigma_f + \boldsymbol{\delta} \sigma_h^{tr} \tag{23}$$

$$\boldsymbol{\varepsilon}^p = \boldsymbol{\varepsilon}_t^{\boldsymbol{p}} + \frac{3}{2} \Delta\varepsilon_p \frac{(\boldsymbol{\sigma}')^{tr}}{\sigma_e^{tr}} \tag{24}$$

$$\boldsymbol{\varepsilon}^e = \boldsymbol{\varepsilon} - \boldsymbol{\varepsilon}^p \tag{25}$$

where σ_h is the hydrostatic stress and $\boldsymbol{\delta}$ is the Kronecker delta.

The final step involves the computation of the consistent material Jacobian $\boldsymbol{C}^{ep} = \partial\Delta\boldsymbol{\sigma}/\partial\Delta\boldsymbol{\varepsilon}$:

$$\dot{\boldsymbol{\sigma}} = \left(K - \frac{2}{3}\mu \frac{\sigma_f}{\sigma_e^{tr}} \right) \boldsymbol{\delta} \, \mathrm{tr}\,(\dot{\boldsymbol{\varepsilon}}) + \left(2\mu \frac{\sigma_f}{\sigma_e^{tr}} + \left(\frac{E_t}{1 + E_t/(3\mu)} - 3\mu \frac{\sigma_f}{\sigma_e^{tr}} \right) \frac{(\boldsymbol{\sigma}')^{tr}}{\sigma_e^{tr}} \frac{(\boldsymbol{\sigma}')^{tr}}{\sigma_e^{tr}} \right) \dot{\boldsymbol{\varepsilon}} \tag{26}$$

where K is the bulk modulus. One should note that if a large strain version is used, an additional initial step should be introduced, which involves rotating the stress, elastic strains and plastic strain tensors according to the Hughes and Winget (1980) algorithm.

4. Usage of the UMAT subroutine

The UMAT subroutine file, `UMATPlasticity.f`, is suitable for both plane strain and 3D analyses without any modifications. As with all UMAT subroutines, the process of creating the model in ABAQUS/CAE is identical to standard models using ABAQUS's in-built except for the material definition. Namely, one has to select "General: Depvar" and "General: User Material" in the "Edit Material" window. In the user material definition one should include 4 mechanical constants (properties), these are described in Table 1. Also, state variables need to be defined for visualisation and storing history dependent variables. For 2D models, a total of 9 solution dependent state (SDV) variables are defined while 13 are required for 3D analyses; these are respectively given in Tables 2 and 3.

PROPS	Variable
1	E - Young's modulus
2	ν - Poisson's ratio
3	σ_Y - Yield stress
4	N - Strain hardening exponent

Table 1: List of user defined material properties (mechanical constants).

SDVs	Variable
1	ε^e_{11} - xx component of the elastic strain tensor
2	ε^e_{22} - yy component of the elastic strain tensor
3	ε^e_{33} - zz component of the elastic strain tensor
4	ε^e_{12} - xy component of the elastic strain tensor
5	ε^p_{11} - xx component of the plastic strain tensor
6	ε^p_{22} - yy component of the plastic strain tensor
7	ε^p_{33} - zz component of the plastic strain tensor
8	ε^p_{12} - xy component of the plastic strain tensor
9	ε_p - equivalent plastic strain

Table 2: List of solution dependent state variables for plane strain models.

Hence, for the case of a 2D model and a material with Young's modulus $E = 200000$ MPa, Poisson's ratio $\nu = 0.3$, initial yield stress $\sigma_y = 600$ MPa, and strain hardening exponent $N = 0.2$, the input file reads:

```
*Material, name=Material-1
     9,
1, EE11, EE11
2, EE22, EE22
3, EE33, EE33
4, EE12, EE12
5, EP11, EP11
6, EP22, EP22
7, EP33, EP33
8, EP12, EP12
9, PEEQ, PEEQ
*User Material, constants=4
200000., 0.3, 600., 0.2
```

SDVs	Variable
1	ε_{11}^{e} - xx component of the elastic strain tensor
2	ε_{22}^{e} - yy component of the elastic strain tensor
3	ε_{33}^{e} - zz component of the elastic strain tensor
4	ε_{12}^{e} - xy component of the elastic strain tensor
5	ε_{13}^{e} - xz component of the elastic strain tensor
6	ε_{23}^{e} - yz component of the elastic strain tensor
7	ε_{11}^{p} - xx component of the plastic strain tensor
8	ε_{22}^{p} - yy component of the plastic strain tensor
9	ε_{33}^{p} - zz component of the plastic strain tensor
10	ε_{12}^{p} - xy component of the plastic strain tensor
11	ε_{13}^{p} - xz component of the plastic strain tensor
12	ε_{23}^{p} - yz component of the plastic strain tensor
13	ε_{p} - equivalent plastic strain

Table 3: List of solution dependent state variables for plane strain models.

Including the name of the state variables in the input file facilitates visualisation. To run the user subroutine one should type in the Abaqus command window:

```
abaqus job=Job-1 user=UMATPlasticity.f
```

where `Job-1` is the name of the input file (Job-1.inp). Some Windows users running old versions of Abaqus or Fortran compilers might have to change the extension of the user subroutine to `.for` (`UMATPlasticity.for`).

A representative input file is provided as an example. The input file models a fracture experiment in a so-called Compact Tension specimen, modelling both the sample and the pins and their interactions (contact). The geometry, mesh and representative results are given in Fig. 2.

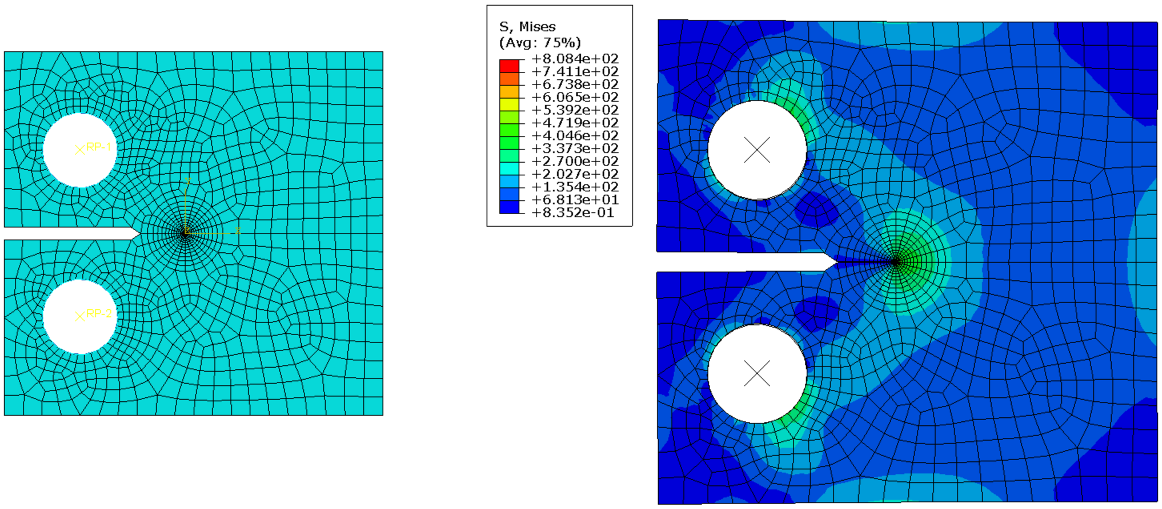

Figure 2: Representative example: Compact Tension specimen, (a) mesh, and (b) von Mises effective stress contours (in MPa).

5. Concluding remarks

The present document accompanies the subroutine `UMATPlasticity.f`, which is provided as supplementary data for the paper (Martínez-Pañeda et al., 2019b). The reader is referred to www.empaneda.com/codes for other examples of user subroutines in ABAQUS. Namely: (1) user element (UEL) subroutines for implementing phase field fracture (Martínez-Pañeda et al., 2018) and fatigue (Kristensen and Martínez-Pañeda, 2020), (2) USDFLD subroutine for implementing functionally graded materials (Martínez-Pañeda and Gallego, 2015; Martínez-Pañeda, 2019), (3) user element (UEL) subroutines for implementing cohesive zone elements (del Busto et al., 2017), (4) user material subroutines for implementing CMSG plasticity theory (Martínez-Pañeda and Betegón, 2015), and (5) user element (UEL) subroutines for implementing higher order strain gradient plasticity (Martínez-Pañeda et al., 2019a).

6. Acknowledgements

E. Martínez-Pañeda acknowledges financial support from Wolfson College Cambridge (Junior Research Fellowship) and from the Royal Commission for the 1851 Exhibition through their Research Fellowship programme (RF496/2018).

References

del Busto, S., Betegón, C., Martínez-Pañeda, E., 2017. A cohesive zone framework for environmentally assisted fatigue. Engineering Fracture Mechanics 185, 210–226.

Dunne, F., Petrinic, N., 2005. Introduction to Computational Plasticity. Oxford University Press, Oxford, UK.

Hughes, T.J.R., Winget, J., 1980. Finite rotation effects in numerical integration of rate constitutive equations arising in large-deformation analysis. International Journal for Numerical Methods in Engineering 15, 1862–1867.

Kristensen, P.K., Martínez-Pañeda, E., 2020. Phase field fracture modelling using quasi-Newton methods and a new adaptive step scheme. Theoretical and Applied Fracture Mechanics 107, 102446.

Martínez-Pañeda, E., 2019. On the Finite Element Implementation of Functionally Graded Materials. Materials 12, 287.

Martínez-Pañeda, E., Betegón, C., 2015. Modeling damage and fracture within strain-gradient plasticity. International Journal of Solids and Structures 59, 208–215.

Martínez-Pañeda, E., Cuesta, I.I., Peñuelas, I., Díaz, A., Alegre, J.M., 2016. Damage modeling in Small Punch Test specimens. Theoretical and Applied Fracture Mechanics 86A, 51–60.

Martínez-Pañeda, E., Deshpande, V.S., Niordson, C.F., Fleck, N.A., 2019a. The role of plastic strain gradients in the crack growth resistance of metals. Journal of the Mechanics and Physics of Solids 126, 136–150.

Martínez-Pañeda, E., Fuentes-Alonso, S., Betegón, C., 2019b. Gradient-enhanced statistical analysis of cleavage fracture. European Journal of Mechanics - A/Solids 77, 103785.

Martínez-Pañeda, E., Gallego, R., 2015. Numerical analysis of quasi-static fracture in functionally graded materials. International Journal of Mechanics and Materials in Design 11, 405–424.

Martínez-Pañeda, E., Golahmar, A., Niordson, C.F., 2018. A phase field formulation for hydrogen assisted cracking. Computer Methods in Applied Mechanics and Engineering 342, 742–761.

Martínez-Pañeda, E., Niordson, C.F., 2016. On fracture in finite strain gradient plasticity. International Journal of Plasticity 80, 154–167.